A GENUINELY MULTIDISCIPLINARY JOURNAL

CHEMPLUSCHEM

CENTERING ON CHEMISTRY

# Accepted Article

**Title:** The Conundrum of α- and β-lapachone Isomerization in Acidic Media: Insights from Experimental and Implicit/Explicit Solvation Approaches

**Authors:** Maicon Delarmelina, Caroline D. Nicoletti, Marcela C. de Moraes, Debora O. Futuro, Michael Buehl, Fernando de C. da Silva, Vitor F. Ferreira, and José Walkimar de M. Carneiro



**To be cited as:** *ChemPlusChem* 10.1002/cplu.201800485

**Link to VoR:** http://dx.doi.org/10.1002/cplu.201800485

A Journal of

ChemPubSoc Europe

WILEY-VCH

www.chempluschem.org

10.1002/cplu.201800485

WILEY-VCH

FULL PAPER

# The Conundrum of α- and β-lapachone Isomerization in Acidic Media: Insights from Experimental and Implicit/Explicit Solvation Approaches

Maicon Delarmelina,[a] Caroline D. Nicoletti,[b] Marcela C. de Moraes,[a] Debora O. Futuro,[b] Michael Bühl,[c] Fernando de C. da Silva,[a] Vitor F. Ferreira,[a],[b] José W. de M. Carneiro*[a]

**Abstract:** Combined experimental and mixed implicit/explicit solvation approaches were employed to obtain insights into the origin of the switchable regioselectivity of acid-catalyzed lapachol cyclization and α-/β-lapachone isomerization. We found that solvating species under distinct experimental conditions stabilized α- and β-lapachone differently, thus altering the identity of the thermodynamic product. The energy profile for lapachol cyclization revealed that this process can occur with low free-energy barriers (lower than 8.0 kcal mol$^{-1}$). For α/β isomerization in a dilute medium, the computed enthalpic barriers are 15.1 kcal mol$^{-1}$ ($\alpha \rightarrow \beta$) and 14.2 kcal mol$^{-1}$ ($\beta \rightarrow \alpha$). These barriers are reduced in concentrated medium to 11.5 and 12.6 kcal mol$^{-1}$, respectively. Experimental determination of isomers ratio was quantified by HPLC and NMR measurements. These findings provide insights into the chemical behavior of lapachol and lapachone derivatives in more complex environments.

## Introduction

Lapachol (**1**) and its pyran derivatives α- and β-lapachone (**5** and **6**, Figure 1) have been known for more than a century due to their potential cytotoxic activity. Today they still rank as one of the most important classes of natural naphthoquinone derivatives studied as anticancer agents.[1-3] Both isomeric forms of lapachone can be prepared by the acid-catalyzed intramolecular cyclization of lapachol. This process is commonly described by the protonation of the alkene group in the aliphatic chain of lapachol (**1**, Figure 1), followed by the intramolecular nucleophilic attack of the hydroxyl group (affording α-lapachone, **5**) or the carbonyl group in position 4 of the quinone ring onto the carbocationic center (affording β-lapachone, **6**).[4]

Interestingly the regioselectivity of this transformation can be controlled by the choice of the Brönsted acid and/or its concentration in aqueous solution, as extensively reported by previous studies.[5,6] When used in a dilute acidic solution, lapachol most commonly affords a mixture of α- and β-lapachone, whereas in concentrated sulfuric acid, β-lapachone is mostly obtained. Likewise, the isomerization equilibrium between α- and β-lapachone favors the formation of the α-isomer in dilute acidic conditions, while the β-isomer is favored in concentrated sulfuric acid. Such switchable regioselectivity has been known since the earlier reports of these derivatives by Paternó, Hooker and Ettlinger.[7-10] Since then, this switch of acid strength has been the standard methodology, with small adaptations, for the preparation of a large set of α- and β-lapachone derivatives. Some interesting experimental variations include the use of 5-substituted lapachol derivatives and Lewis acid catalysts.[11,12]

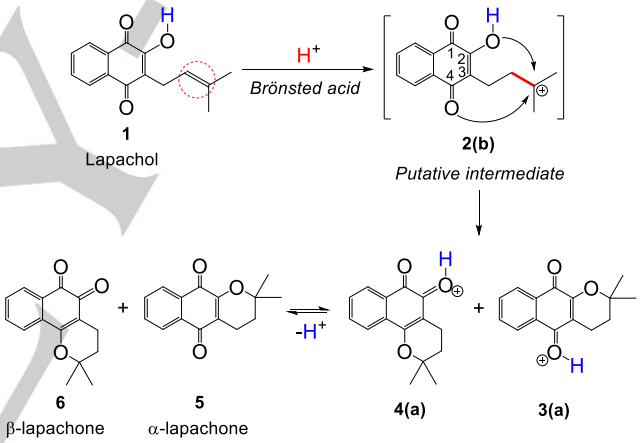


**Figure 1.** Commonly proposed path for the formation of α- and β-lapachone (**5** and **6**) via the carbocation intermediate **2(b)**.

Despite its simplicity, the prototypical mechanism (Figure 1) is unable to explain the intriguing feature of the switchable regioselectivity of lapachol. Furthermore, based only on the relative stabilities of the α- and β-isomers, it is impossible to correctly predict such behavior. Herein, we report a combined computational and experimental effort to describe the relative stabilities of the isomeric lapachones under distinct acidic conditions. Going beyond the known limitations of implicit solvation schemes, mixed implicit/explicit solvation models, built by explicitly incorporating different bases as proton acceptors in the computations, allowed us to identify how the interactions between lapachone and the predominant solvating species can affect the stability of α- and β-lapachone, resulting in the observed regioselectivity.

[a] Dr. M. Delarmelina, Prof. Dr. M. C. de Moraes, Prof. Dr. F. C. da Silva, Prof. Dr. V. F. Ferreira, Prof. Dr. J. W. M. Carneiro
Instituto de Química
Universidade Federal Fluminense
Niterói, Rio de Janeiro 24020-141 (Brazil)
E-mail: jose_walkimar@id.uff.br
[b] C. D. Nicoletti, Prof. Dr. D. O. Futuro, Prof. Dr. V. F. Ferreira
Faculdade de Farmácia
Universidade Federal Fluminense
Niterói, Rio de Janeiro 24241-002 (Brazil)
[c] Prof. Dr. M. Bühl
University of St Andrews
School of Chemistry
North Haugh
St Andrews, Fife KY16 9ST (Scotland (UK))

Supporting information for this article is given via a link at the end of the document.

## Results and Discussion

As it will be demonstrated later on, the peculiar switchable regioselectivity of lapachol cyclization and lapachone isomerization in acidic media can only be described by computational approaches if explicit solvation is incorporated into the computations. To gain deeper insights into the process, we will first present the interaction of the lapachones with the different species expected to be present in the reaction mixture under different acidic conditions. After that, we will discuss the possible mechanisms involved in the chemical transformations.

In the present study, we initially computed the relative energies of α- and β-lapachone (**5** and **6**) within the implicit solvation approach IEFPCM (Integral Equation Formalism PCM), using water as solvent and considering both neutral and protonated states of the lapachones (see Figure S29 and S30 for the quantification of the proton affinity and basicity of α- and β-lapachone). In their neutral states, α-lapachone (**5**, Figure 2a) is more stable than β-lapachone (**6**, Figure 2a). However, β-lapachone turns into the more stable isomer after protonation of the carbonyl group $C_2$=O ($C_4$=O for the α-isomer) (**4(a)**, Figure 2b). In agreement with Ettlinger's early findings,[10] DFT results within the implicit solvation approach show that β-lapachone has a higher basicity than the α-isomer.

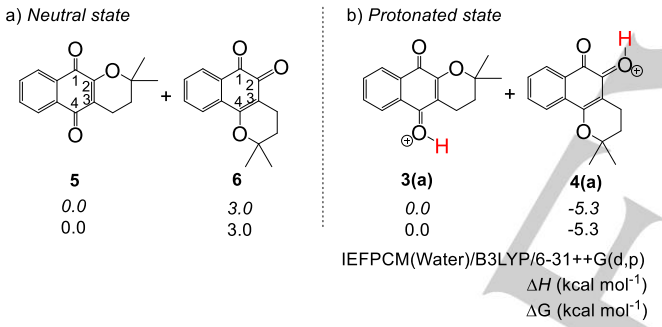


**Figure 2.** Relative energies of α- and β-lapachone in their (a) neutral and (b) protonated states.

This behavior can be rationalized in terms of the higher electron density in the region between the two carbonyl groups $C_1$=O and $C_2$=O in β-lapachone due to the lone electron pairs occupying $sp^2$-like orbitals in these groups. Charge concentration around them destabilizes the neutral state of β-lapachone when compared to α-lapachone, while its protonated state is largely stabilized due to the electron-withdrawing effect of the proton bonded to the $C_2$=O group and the intramolecular hydrogen bond formed with the neighboring $C_1$=O carbonyl group.[13] Accordingly, β-lapachone (or protonated β-lapachone **4a**) would be the thermodynamic product in the acid-catalyzed cyclization of lapachol. As for the major formation of α-lapachone in dilute acid, Ettlinger[10] reasoned that α-lapachone precipitates, shifting the chemical equilibrium towards the α-isomer and thus consuming the formed β-lapachone. Our own experiments in dilute sulfuric and hydrochloric/acetic acid, however, afforded a more refined picture, as shown by the results summarized in Figure 3.

When using solutions of dilute hydrochloric/acetic or sulfuric acid at low concentrations (HCl/AcOH: 18% and 9%; $H_2SO_4$: 25% and 50%, Figure 3, Entries A, C, E and G), product precipitation was not observed in lapachol cyclization, and a mixture of α- and β-lapachone was obtained. Additionally, for the experiments at higher temperature (60 ºC, Figure 3, Entries B, D, F and H), when compared to the analogues reactions performed at room temperature, α-lapachone is clearly obtained as the thermodynamic product (71-98% of α-lapachone was obtained). Longer reaction times corroborate these observations, as the amount of α-lapachone increases after 48 hours (79-98% of α-lapachone was obtained). Moreover, when pure α-lapachone was solubilized in dilute HCl/AcOH (Table 1) no interconversion into β-lapachone was observed. Pure β-lapachone was also solubilized in dilute sulfuric acid (Table 1), and the conversion of β- into α-lapachone was rapidly observed after 10 minutes, which continued occurring after 24 hours.

On the other hand, β-lapachone was obtained as major product for reactions using sulfuric acid at concentrations of 75% or higher (86-100% of β-lapachone was obtained, Figure 3, Entries I and J). Additionally, the interconversion of α- into β-lapachone in concentrated sulfuric acid was indicated by the almost instantaneous change of the solution from a yellowish to dark red color. Under these conditions, β-lapachone is, arguably, the thermodynamic product.

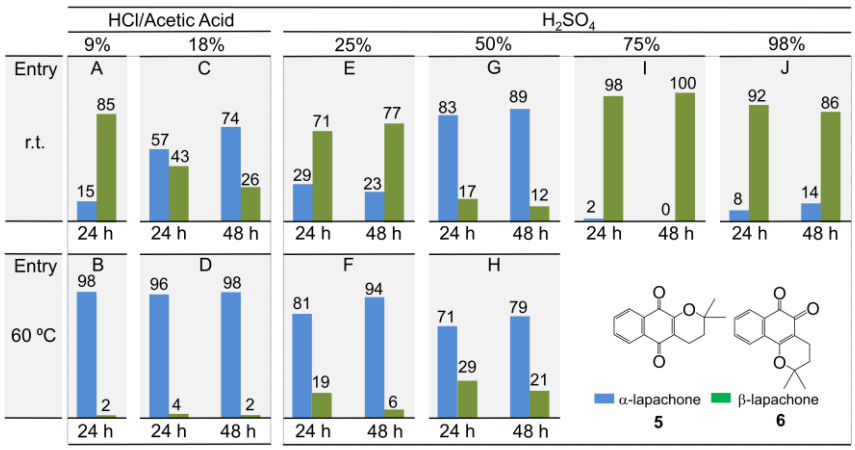


**Figure 3.** Percentages of α- and β-lapachone obtained under distinct reaction conditions and determined by HPLC analysis.

**Table 1.** Percentages of α- and β-lapachone obtained after the solubilization of α-lapachone in solutions of 18% HCl/AcOH at room temperature (Entries A-D) and after the solubilization of β-lapachone 53% $H_2SO_4$ at 60 ºC (Entries E-G).

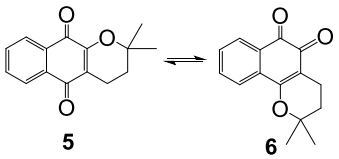

**5** **6**

| Entry | Temperature | Solvent | Time | **5** : **6** |
|---|---|---|---|---|
| A | r.t. | HCl/AcOH 9% | 0 h | 100% : 0% |
| B | r.t. | HCl/AcOH 9% | 24 h | No reaction |
| C | r.t. | HCl/AcOH 18% | 0 h | 100% : 0% |
| D | r.t. | HCl/AcOH 18% | 24 h | No reaction |
| E | 60 ºC | $H_2SO_4$ 53% | 0 h | 0% : 100% |
| F | 60 ºC | $H_2SO_4$ 53% | 10 min | 26% : 74% |
| G | 60 ºC | $H_2SO_4$ 53% | 24h | 45% : 55% |

**Table 2.** Percentages of α- and β-lapachone obtained for the cyclization of lapachol in $CH_2Cl_2$ and $HCl_{(g)}$.

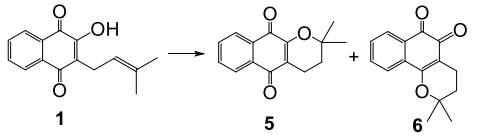

**1** **5** **6**

| Entry | Temperature | Solvent | Time | **5** : **6** |
|---|---|---|---|---|
| A | r.t. | $HCl_{(g)}$, $CH_2Cl_2$ | 24 h | 7% : 93% |
| B | r.t. | $HCl_{(g)}$, $CH_2Cl_2$ | 48 h | 8% : 92% |

In a last experimental test, lapachol cyclization was also performed using $HCl_{(g)}$ in a 1,2-dichloromethane solution (Table 2), where the effect of other protic species present in the reaction mixture is absent. Interestingly, in this case, β-lapachone was obtained almost exclusively. From the analysis of the isomer ratio in all of the aforementioned experimental conditions and by excluding the solubility of the final product as a determining factor for the regioselectivity of lapachol cyclization, we conclude that the relative stability of lapachone isomers is significantly modified by the environment in which the reaction is performed.

It is noteworthy that the only diverging experimental results were observed for the cyclization of lapachol at room temperature in the most dilute solutions (HCl/AcOH 9% and $H_2SO_4$ 25%, Entries A and E, Figure 3), in which β-lapachone was obtained as the major product. In these cases, lapachol could not be completely solubilized, as was confirmed by the high amount of lapachol still detected in the HPLC chromatograms for these reaction conditions (Figures S1 and S7, Supporting Information). Most likely, the cyclization process proceeds via a different mechanism from that prevailing under the aforementioned reaction conditions. More details on such an alternative mechanism are given in the following subsections.

Recalling the initial results from the DFT calculations (Figure 2), it is clear that the implicit solvation approach alone is unable to mimic the different reaction conditions and therefore the distinguishable stability of the lapachones. In fact, the inability of these schemes to reproduce such a chemical environment is not surprising, as they ignore specific intermolecular interactions between the solute and solvent, which may be of great relevance in derivatives containing a large number of polar interacting sites, such as is the case for the quinone derivatives.[14]

Improvement of the chemical description of lapachones within such an approach can be reached by explicitly including the effect of solvent molecules close to the polar sites of the quinone core. This is especially useful when dealing with charged solutes and proton transfer processes, which is the case for lapachol cyclization and lapachone isomerization. Despite the limitations of such a static approach for the investigation of reactions in the condensed phase, a myriad of previous studies has successfully employed explicitly solvated systems embedded into a dielectric continuum for a reasonable description of systems displaying strong solute–solvent interactions in organic, biological, and organometallic reactions.[15-22] It is well known, however, that care needs to be taken in choosing the structural configuration with the lowest energy and in the analysis of the energy profiles computed for such transformations.

*Construction of the microsolvation model*

In any of the acidic solutions indicated in Figure 3 and in Tables 1 and 2, the lapachones can be expected to exist in their protonated state. Based on this assumption, the construction of the microsolvation models was divided into three steps: (i) computation of the proton affinities of all of the basic sites of lapachone; (ii) microsolvation of the protonated site; and (iii) microsolvation of other polar sites. The most probable solvating species were hypothesized based on the identity and concentration of the acid used in each experiment as well as on previous investigations of proton transfer mechanisms in hydrochloric and sulfuric acid solutions, as detailed next.

For a dilute acidic solution, the formation of ion-pairs of the type $H_3O^+\cdots(H_2O)_n\cdots B^-$ ($B^-$ = $Cl^-$, $HSO_4^-$ or $SO_4^{2-}$) is expected, in which proton transfer is mediated by one or more water molecules.[23-26] According to this hypothesis, the protonation of lapachones in a dilute acidic solution can be pictured as occurring by the formation of a hydronium ion, followed by proton transfer to one of the basic sites of lapachone. For the purpose of constructing a microsolvation model, the remaining water molecule has to be kept as the solvating species on the protonated site, as shown in Figure 4(a).

Two possible hydrogen bond donors were considered for describing the microsolvation of the other polar site of the lapachones, as they are abundantly found in dilute solutions: water molecules and the hydronium ion itself. The most reasonable structural configurations for such lapachone···solvating-species interactions were evaluated (see Figures S31 and S32), and the most stable ones were selected for comparison of the relative energies of the two isomers (Figure 4(b-c)). Free-energies were computed at a higher pressure to model the condensed phase (see Computational Details).

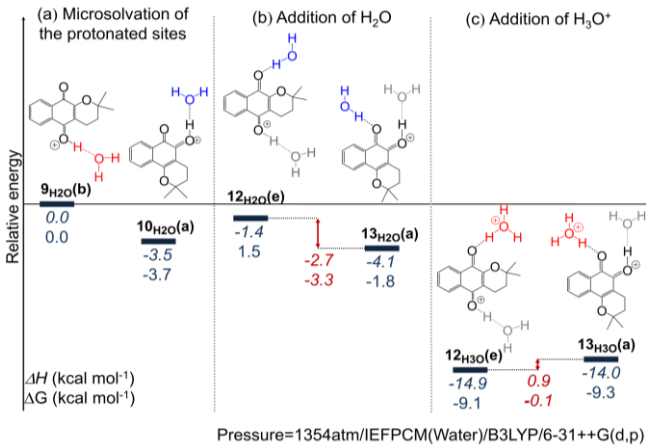


**Figure 4.** Relative energies of α- and β-lapachone considering (a) only the microsolvation of protonated sites, solvation of the protonated site plus (b) a second water molecule or (c) a hydronium ion. The scale of the given graphic is based on relative enthalpy values. Values in red show the energy difference between α- and β-isomers within the same microsolvation model.[27]

The **$9_{H2O}$(b)/$10_{H2O}$(a)** and **$12_{H2O}$(e)/$13_{H2O}$(a)** pairs (Figures 4(a) and 4(b)) roughly presented the same relative energy trends as those obtained by using the implicit models (Figure 2(b)), *i.e.,* β-lapachone is more stable than α-lapachone. However, when we considered microsolvated systems **$12_{H3O}$(e)/$13_{H3O}$(a)** (Figure 4(c)), with the hydronium ion solvating a second polar site of the lapachones, a significant drop in the relative energy is observed for the α-isomer. Now both systems present a much smaller energy difference of approximately 0.9 kcal mol$^{-1}$ for the relative enthalpy. More interestingly, when their relative enthalpies are compared, protonated α-lapachone is found to be more stable than protonated β-lapachone. As shown in Figure S40, these results are independent of the DFT functional used for the energy calculation.

The energy of the interaction between $H_3O^+$ and the $C_1$=O carbonyl group in **$12_{H3O}$(e)** and **$13_{H3O}$(a)** were computed as -24.0 and -17.9 kcal mol$^{-1}$ (Figure S39, Supplementary Material), respectively, consistent with the formation of a strong hydrogen bond between those species. The relatively short $C_1$=O···H distances observed for the optimized structures (1.30 and 1.33 Å for **$12_{H3O}$(e)** and **$13_{H3O}$(a)**, respectively) also confirmed such strong interactions. Despite the short $C_1$=O···H distances, the proton is still formally bonded to the "$H_2O$" molecule. When the proton was manually transferred to the $C_1$=O group, it afforded a less stable structure or, in some cases, the proton migrated back to the solvent molecule during the optimization process.

Additional hydrogen bond donor species solvating other lone pairs of the carbonyl groups were not considered for further analysis, as such interactions always resulted in C=O···H distances longer than 2.0 Å, presenting only weak dipole-dipole interactions. Moreover, interactions between hydrogen bond donors and the lone pairs of the oxygen atom in the pyran ring of the lapachones always led to either the solvent molecule moving away during the optimization process or increasing the energy of the system.

The possibility of protonated acetic acid mediating the proton transfer process was also considered, however, the microsolvated system composed of **$12_{H3O}$(e)/$13_{H3O}$(a)** was still the most adequate for describing the dilute acidic conditions (See Figure S37 for a more detailed discussion).

A similar explicit solvation model was used for describing the concentrated sulfuric acid medium. For this case, the low water concentration may allow the presence of different species in the reaction mixture, other than the water molecules themselves, to assist the proton transfer.

Previous studies showed that in highly concentrated solutions of sulfuric acid (between 75 and 100%), high contents of undissociated $H_2SO_4$ and $HSO_4^-$ are observed (over 73% of undissociated $H_2SO_4$).[28] Furthermore, investigations of the proton transfer mechanism in sulfuric acid solutions using $(H_2SO_4)_n\cdots(H_2O)_m$ clusters have shown that, at low water concentrations, the assistance of non-deprotonated $H_2SO_4$ is mandatory for the stabilization of the conjugate base $HSO_4^-$ and allows deprotonation to occur.[29] According to this hypothesis, the proton would be transferred via a $H_2SO_4\cdots H_2SO_4\cdots$B cluster, in which B is any base or solvent molecule present in the mixture capable of accepting the proton.[30]

Accordingly, the $[H_2SO_4\cdots H_2SO_4]$ dimer was initially considered as the proton donor for proton transfer to the lapachones in a concentrated acid solution. After proton transfer to one of the basic sites of lapachone, the remaining species, the $[H_2SO_4\cdots HSO_4^-]$ anion, was kept as the solvating species of the protonated site (Figure 5(a)). Additionally, a second $[H_2SO_4\cdots H_2SO_4]$ dimer was used as the hydrogen bond donor for the solvation of additional polar sites of the lapachones. The configuration search for all clusters containing $[H_2SO_4\cdots HSO_4^-]$ and $[H_2SO_4\cdots H_2SO_4]$ is shown in Figures S34-S36 (only the most stable ones are shown here).

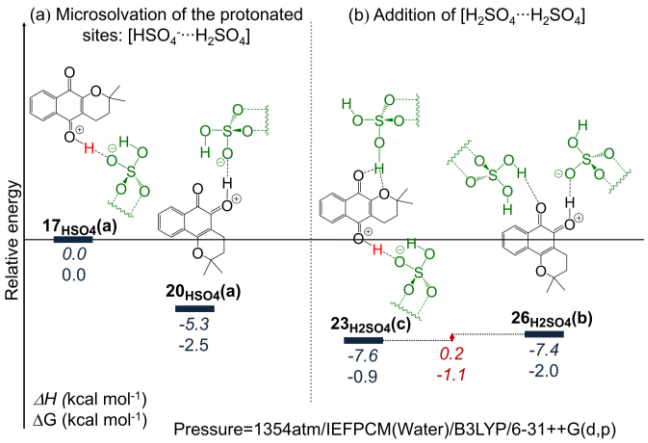


**Figure 5.** Relative energies of α- and β-lapachone considering the microsolvation model constructed using $HSO_4^-/H_2SO_4$ as the solvating species. The scale of the given graphic is based on relative enthalpy values. Values in red show the energy difference between α- and β-isomers within the same microsolvation model.[27]

The result of such lapachone/$[H_2SO_4\cdots HSO_4^-]$/$[H_2SO_4\cdots H_2SO_4]$ complexes is that the relative energy of the pair **$23_{H2SO4}$(c)/$26_{H2SO4}$(b)** (Figure 5(b)) decreased significantly by approximately 7-8 kcal mol$^{-1}$ when compared to the reference system. Moreover, it is worth noticing that the difference between the $C_1$=O···HBD interaction energy in α-lapachone (**$23_{H2SO4}$(c)**)

and β-lapachone (**26$_{H2SO4}$(b)**) is now only 1.6 kcal mol$^{-1}$ (Figure S39, Supporting Information). The relative enthalpy computed for the pair **23$_{H2SO4}$(c)/26$_{H2SO4}$(b)** is quite similar and presented a variation of only 0.2 kcal mol$^{-1}$. Conversely, the relative free-energy computed for this pair presents β-lapachone as more stable than α-lapachone by 1.1 kcal mol$^{-1}$. In this case, the computed free-energies are consistent with the experimental observations for the reactions in sulfuric acid at higher concentrations (Figure 3, Entries I and J), where β-lapachone is the expected thermodynamic product.

Care was taken in the choice of the supermolecule used for this comparison so that the solvating species would not interact significantly between themselves and only their effect on the naphthoquinone core would be computed. However, it is worth noting that microsolvated β-lapachone **26$_{H2SO4}$(b)** can still be obtained in other configurations, for which its relative energy would be additionally reduced by intermolecular interactions between the solvent molecules (see Figure S36, Supporting Information). Despite the entropic penalty expected for forming such a highly organized configuration, the drop in the enthalpy would still be enough to significantly reduce the relative free-energy of these systems. This possibility, although not considered for this discussion, reinforces our argument that the interaction between β-lapachone and [$H_2SO_4$···$H_2SO_4$] fragments results in β-lapachone being more stable than α-lapachone under these conditions.

In solutions of sulfuric acid at concentrations of 75% or more,[28] undissociated $H_2SO_4$ is expected to be present. It is also at these high concentrations that β-lapachone starts to be experimentally obtained as the major product (Figure 3, Entries I and J). From such observation, it is reasonable to expect that the presence of undissociated $H_2SO_4$ and its interaction with the lapachone can be involved in the preferential formation of β-lapachone, as also suggested by our microsolvated system **23$_{H2SO4}$(c)/26$_{H2SO4}$(b)**.

A final analysis on the effects of the hydrogen bond donors and acceptors (HBD and HBA) revealed that the hydrogen bond acceptors $H_2O$ and [$H_2SO_4$···$HSO_4^-$] affect the relative energy of the system only weakly, changing the relative free energies by less than 1 kcal mol$^{-1}$ when the [$H_2SO_4$···$HSO_4^-$] dimer is replaced by $H_2O$ (Figure S38, Supporting Information). Comparison of the strength of the $C_1$=O···HBD interaction in the pairs **12$_{H2O}$(e)/13$_{H2O}$(a)** and **23$_{H2SO4}$(c)/26$_{H2SO4}$(b)** (Figure S38, Supporting Information) revealed that this interaction is weaker in β-lapachone than in α-lapachone. The protonated site in β-lapachone ($C_2$=O), being spatially closer to $C_1$=O than in α-lapachone, results in a neighboring positive charge at the protonated $C_2$=O and a weaker $C_1$=O···HBD interaction for β-lapachone. Additionally, beyond the expected stabilization from the $C_1$=O···HBD interaction, α-lapachone is further stabilized by a weak dipole-dipole interaction between $H_3O^+$ and O(pyran) in **12$_{H2O}$(e)** (where the $H_2O^+$-H···O(pyran) distance amounts to 2.432 Å). By comparison of conformers **12$_{H3O}$(e)** and **12$_{H3O}$(f)** (Figure S32, Supporting Information), it appears that such interaction further decreases the energy of α-lapachone by circa 2 kcal mol$^{-1}$.

Overall, two microsolvated lapachone systems were identified, to which the experimental regioselectivity of the acid-catalyzed cyclization of lapachol can be directly compared. By combining $H_2O$ and $H_3O^+$ as hydrogen bond acceptor and donor, respectively, we were able to mimic the stability of the protonated lapachones in dilute acidic conditions. Meanwhile, the reversed stability of the protonated lapachones observed in highly concentrated sulfuric acid was reproduced by using [$H_2SO_4$···$HSO_4^-$] and [$H_2SO_4$···$H_2SO_4$] dimers as hydrogen bond acceptor and donor, respectively. With these microsolvation models in hands, we used these to explore the energy profiles of lapachol cyclization and lapachone isomerization, as discussed next.

*Lapachol protonated states and microsolvation*

Similar to the approach used for the lapachones, the proton affinity and basicity of lapachol were also analyzed for this stage. Three possible protonation sites on lapachol were considered: (i) the carbonyl group in position 1; (ii) the alkene group in the aliphatic chain; and (iii) the carbonyl group in position 4. All the possible conformers for the protonated state of lapachol were considered (Figures S27 and S28), and the most stable one in each case was chosen for calculation of the enthalpy and Gibbs free-energy changes for the protonation process (Figure 6).

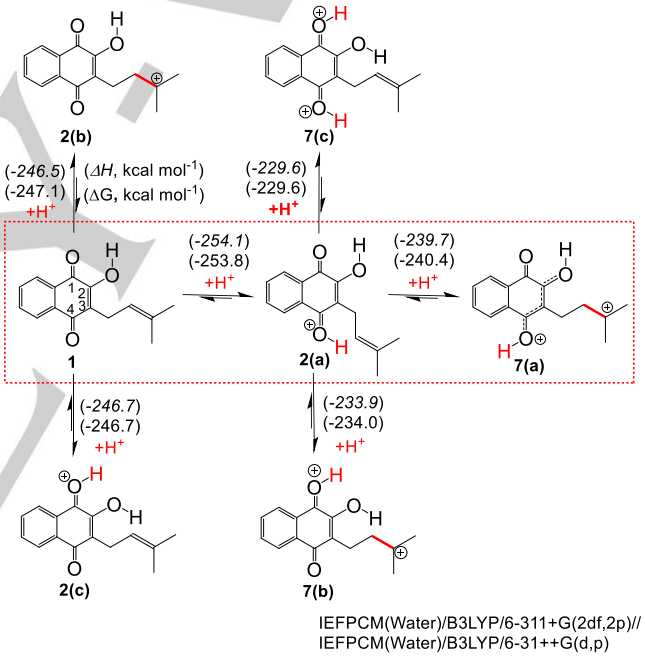


**Figure 6.** Energy changes for the mono- and diprotonation of lapachol (in kcal mol$^{-1}$ relative to **1**).

According to the prototypical mechanism for lapachol cyclization (Figure 1), the carbocation intermediate (**2(b)**, Figure 6) should be formed from lapachol in acidic medium, which then would undergo intramolecular nucleophilic attack, affording the pyran derivatives. However, the proton affinities suggest that the first protonation of lapachol must occur at the carbonyl group at position 4 (**2(a)**, Figure 6), the most basic site of lapachol. Interestingly, however, the solvation of **2(b)** by $H_2O$ and $H_3O^+$ (Figure 7), as proposed before for dilute acidic conditions, revealed that the presence of the hydronium ion close to carbonyl group $C_4$=O results in proton abstraction from the hydronium ion by the carbonyl group. The resulting structure **8$_{H2O}$(a)** (Figure 7) presents two formal positive

charges separated by an aliphatic chain, a feature that may contribute to the stability of such diprotonated species.

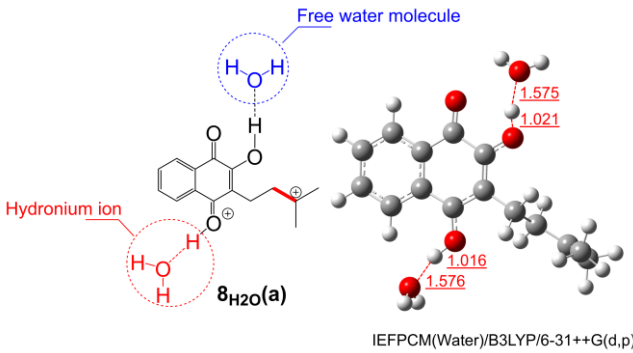


**Figure 7.** Explicit solvation of the diprotonated lapachol **$8_{H2O}$(a)**. Atomic distances are given in Angstroms (Å).

The Gibbs free-energy change for the first and the second protonation differs by 13.4 kcal mol$^{-1}$ (**2a** + $H^+$ → **7a**, Figure 6). Although the second protonation is less exergonic than the first one, its value still seems to allow for the existence of **7(a)** (Figure 6) - or its explicitly solvated analogue **$8_{H2O}$(a)** (Figure 7) - even if at low concentration. Furthermore, species **$8_{H2O}$(a)** is an adequate intermediate for this lapachol cyclization reaction, as it has the carbocation required for cyclization and two very similar nucleophilic sites (the protonated carbonyl group $C_4$=O and the hydroxyl group $C_2$-OH), which is a sound explanation for the observed regioselective cyclization of lapachol. Moreover, **$8_{H2O}$(a)** is a promising candidate for resolving an apparent contradiction in the prototypic mechanism, in which investigation of its energy profile revealed that the β-isomer would be rapidly formed from the carbocationic intermediate **2(b)** in a process with no energy barrier (see Figure S42, Supplementary Material).

Based on our experimental results discussed above, the lapachol cyclization mechanism can still occur via the monoprotonated intermediate **2(b)**, but only under conditions where low acid concentrations are used, as for HCl/AcOH 9% and $H_2SO_4$ 25% (Entries A and E, Figure 3). For such reaction conditions, the absence of a sufficient amount of proton donors allows the formation of monoprotonated lapachol, and the reaction follows the mechanism given in Figure 1. According to this hypothesis, the nucleophilic attack on the carbonyl group $C_4$=O occurs with no enthalpic barrier (as shown in Figure S42, Supplementary Material), and the formation of β-lapachone as the major product can be expected. The reaction performed using $HCl_{(g)}$ in 1,2-dichloromethane solution (Table 2) is expected to behave similarly, with further participation of a second lapachol molecule as a hydrogen bond acceptor in the cyclization process. For the majority of the experimental conditions investigated here, however, the diprotonated intermediate **$8_{H2O}$(a)** (Figure 7) must dominate the cyclization process.

*Lapachol cyclization in dilute acidic medium and in concentrated sulfuric acid*

The energy profile for the cyclization of lapachol was computed (Figure 8) considering the explicit solvation models for dilute acidic medium shown in Figures 4 and 7. Cyclization of the diprotonated lapachol **$8_{H2O}$(a)** was initially evaluated as affording diprotonated lapachones. However, two positive charges are not supported by the O-C=C-C=O conjugated system in the pyran naphthoquinone ring, as optimization of the diprotonated lapachones led to cleavage of the C-O bond and regeneration of **$8_{H2O}$(a)**.The cyclic products could only be obtained upon the addition of one or more water molecules, involving a transition state structure in which one of the hydrogen atoms in the quinone moiety is transferred to one of these water molecules or to the neighboring C(1)=O group in a concerted step (even though this step has a much higher energy barrier, as shown in Figure S43). Hence, the formation of α-lapachone is possible via the nucleophilic attack of the hydroxyl group on the carbocation in the aliphatic chain, followed by a concerted transfer of the hydrogen from the hydroxyl group to a water molecule (**$12_{H3O}$-TS**, Figure 8). In this case, the proton is transferred to the solvent molecule, while the previously formed hydronium ion maintains its interaction with the neighboring $C_1$=O group. Meanwhile, the formation of β-lapachone occurs via intermolecular hydrogen transfer from $C_4$=O to a water molecule (**$13_{H3O}$-TS**, Figure 8). The optimized structures of **$12_{H3O}$-TS** and **$13_{H3O}$-TS** are shown in Figure S44.

The monoprotonated lapachones solvated by one water molecule are shown in Figure 8 as the final products **$9_{H2O}$(b)** and **$10_{H2O}$(a)**. The products **$12_{H3O}$(a)** and **$12_{H3O}$(e)** (Figure 8) are obtained after full optimization, starting from the transition structures **$12_{H3O}$-TS** and **$13_{H3O}$-TS**, respectively, distorted towards the products along the imaginary vibrational mode. The most stable configurations of α- and β-lapachone are **$12_{H3O}$(b)** and **$13_{H3O}$(a)**, for which, based on the enthalpy values, α-lapachone **$12_{H3O}$(b)** was computed as the thermodynamic product.

The higher stability of α-lapachone (**$12_{H3O}$(e)**) and the small energy difference between the isomers agree with the experimental behavior for these systems in dilute acidic media (Figure 3, Entries C and G). Under these conditions, a mixture of α- and β-lapachone is obtained as a consequence of their similar relative energies. Furthermore, the amount of β-lapachone decreases with longer reaction times, as this isomer is slowly converted into the α-isomer, the thermodynamic product under such conditions. The same is valid for the reactions performed at higher temperature (Figure 3, Entries B, D, F and H).

From our findings, we propose that the interconversion mechanism of α- and β-lapachone is connected by the diprotonated lapachol **$8_{H2O}$(a)** and the energy barrier for such conversion is determined by **$13_{H3O}$-TS**, the highest stationary point on the energy profile given in Figure 8. Based on this profile, the computed enthalpy barrier for the interconversion of β-lapachone into α-lapachone is 15.1 kcal mol$^{-1}$, whereas for the interconversion of α- into β-lapachone the enthalpic barrier is 14.2 kcal mol$^{-1}$ (see Supplementary Material for energy barriers computed with a set of DFT functionals, Figure S41 and Table S1).

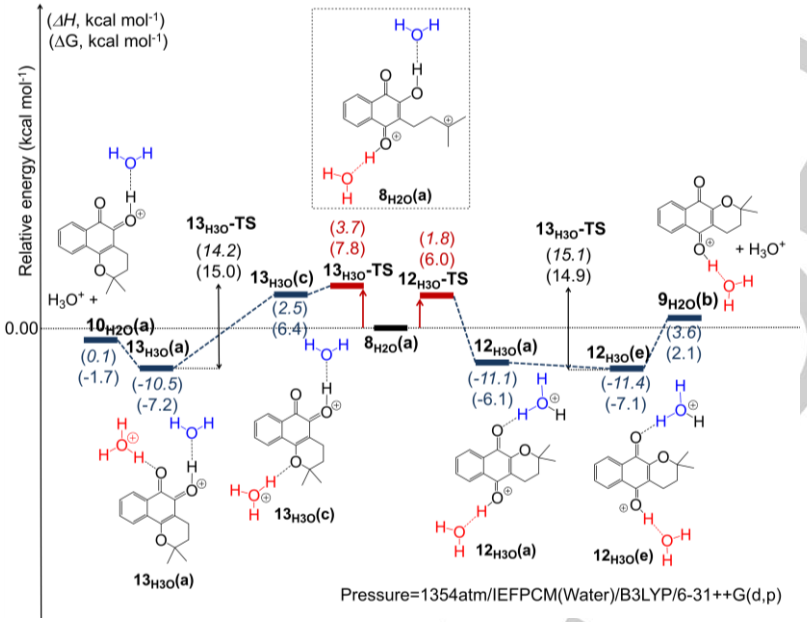


**Figure 8.** Energy profile for the cyclization of explicitly solvated diprotonated lapachol **$8_{H2O}$(a)**. The scale of the given graphic is based on the relative free-energy values. Values in black show the energy barrier for the interconversion of **$12_{H3O}$(e)** and **$13_{H3O}$(a)**.[27]

Computations on the analogous diprotonated lapachol **$8_{HSO4}$(a)** and **$8_{HSO4}$(b)** (Figure 9), constructed within the microsolvation model for concentrated sulfuric acid medium, revealed a very low energy barrier (lower than 0.6 kcal $mol^{-1}$, Figure S45, Supporting Information) for the lapachol cyclization process. According to these results, the energy barrier for the interconversion between α- and β-lapachones is determined by **$8_{HSO4}$(b)**, the highest stationary point on this energy profile. Therefore, the computed enthalpy barrier for interconversion of β-lapachone into α-lapachone (**$26_{H2SO4}$(b)** → **$23_{H2SO4}$(c)**, Figure 9) is 11.5 kcal $mol^{-1}$, whereas for the interconversion of α- into β-lapachone the enthalpy barrier is 11.7 kcal $mol^{-1}$ (**$23_{H2SO4}$(c)** → **$26_{H2SO4}$(b)**, Figure 9). The computed free-energy barriers are 12.6 and 11.5 kcal $mol^{-1}$ for the conversion of β- into α-lapachone and from α- into β-lapachone, respectively.

The smaller free-energy barrier for interconversion of α- into β-lapachone and the higher stability of the β-isomer agrees with the experimental observations for lapachol cyclization in concentrated sulfuric acid (Figure 3, Entries I and J). Additionally, the lower energy barrier for lapachone interconversion in concentrated sulfuric acid (Figure 9), when compared to the values obtained for the dilute acidic medium (Figure 8), are consistent with the almost instantaneous interconversion of α- into β-lapachone observed in highly acidic conditions, whereas the interconversion of β- into α-lapachone in dilute acidic conditions is much slower (Table 1).

## Conclusions

In summary, through a combination of experimental and computational approaches, for the first time we are able to rationalize the acid-catalyzed regioselective formation of α- and β-lapachones from lapachol. On the computational side, a mixed explicit/implicit solvation approach was instrumental for mimicking the distinct acidic conditions investigated here and to properly compute the relative stabilities of the α- and β-isomers. Within the microsolvation models that were constructed, we observed that different hydrogen bond donors (HBDs) present under each reaction condition can distinctly stabilize the lapachones, reducing the energy difference computed for α- and β-isomers relative to that obtained when using implicit solvation schemes only. The identity of the HBD and, consequently, the magnitude of the HBD···α-/β-lapachone interaction, alters the identity of the thermodynamic product in lapachol cyclization when the reactions are performed in either dilute or concentrated acid solutions.

For construction of the microsolvation models, $H_2O/H_3O^+$ and $[H_2SO_4\cdots HSO_4^-]/[H_2SO_4\cdots H_2SO_4]$ species were chosen as H-bond-acceptors/H-bond-donors and used for mimicking a dilute acid solution and a concentrated sulfuric acid medium, respectively. For the dilute acid model, protonated α-lapachone was computed for the first time to be more stable than protonated β-lapachone, with an enthalpy difference of 0.9 kcal $mol^{-1}$. When using the microsolvated system representing the concentrated

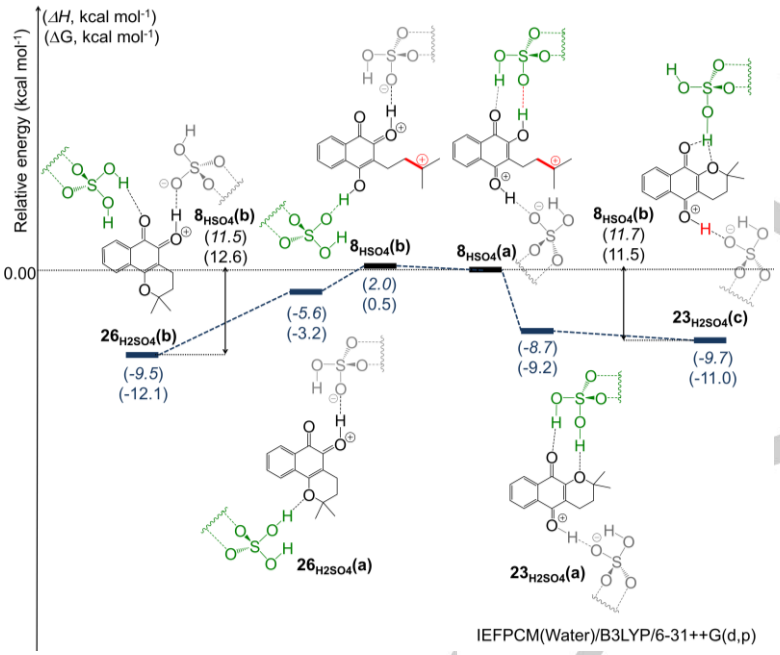


**Figure 9.** Energy profile for the cyclization of explicitly solvated diprotonated lapachols **8$_{HSO4}$(a)** and **8$_{HSO4}$(b)**. The scale of the given graphic is based on the relative free-energy values. Values in black show the energy barrier for the interconversion of **23$_{H2SO4}$(c)** and **26$_{H2SO4}$(b)**.[27]

sulfuric acid medium, protonated β-lapachone was obtained as the most stable isomer. In both cases, our explicit/implicit solvation approach reproduces the experimental trends for the α-/β-lapachone interconversion equilibrium.

From the analysis of the energy profile for lapachol cyclization, a diprotonated lapachol was identified as the key intermediate for both the cyclization process and for the interconversion of the isomeric products. The lapachol cyclization process was computed as occurring with a very low or without an enthalpic barrier. The α/β isomerization process in dilute acid, on the other hand, presented enthalpy barriers of 15.1 kcal mol$^{-1}$ (α → β) and 14.2 kcal mol$^{-1}$ (β → α). The analogous process in concentrated sulfuric acid presented free-energy barriers of 11.5 and 12.6 kcal mol$^{-1}$ for α → β and β → α conversion, respectively.

Despite such small energy differences for the competitive processes in dilute and concentrated acid conditions, we observed that they have a great influence on the isomerization equilibrium of α- and β-lapachone. It is intriguing that the interaction of the hydrogen bond donors with $C_1$=O is mainly responsible for such effect. Moreover, the moderate energy barriers for isomerization calculated here may raise the question whether the same α-/β-lapachone equilibrium shifting would occur in more complex systems, such as biological environments. Evaluation of this possibility, however, maybe a daunting task, as the energy differences, as demonstrated here, can be quite small, although they were significant for changes in the α-/β-lapachone ratio in our own experiments.

## Experimental Section

*1. Experimental details*

**General Procedure for the Preparation Pyranonaphthoquinones Derivatives from Lapachol.** A round-bottom flask was charged with lapachol (100 mg, 0.414 mmols) and 10 mL of acid in different concentrations (as described in Figure 3 and 4). The reaction mixture was kept under magnetic stirring for 48 hours. Half of the reaction mixture was removed during the first 24 hours, the phases were separated and the organic phase was washed with sodium bicarbonate saturated solution (3 x 50 mL), dried with anhydrous sodium sulphate, filtered, and evaporated under reduced pressure. The resulting solids of colours ranging from yellow to red were not separated. The remaining reaction mixture was removed after 48 hours and underwent the same treatment as the first half of the reaction mixture.

**Reaction with neat hydrochloric acid.** A round-bottom flask was charged with Lapachol (50 mg, 0.207 mmol) and sufficient amount of dichloromethane for complete solubilization. External cooling with ice was used and the solution was kept under stirring. Next, gaseous hydrochloric acid, formed by the reaction of sodium chloride and sulfuric acid was bubbled into the solution. Aliquots were removed and treated as described above.

**Determination of α- and β-lapachone ratio by HPLC.** Chromatography system: HPLC-DAD analyses were conducted in a Shimadzu LC System (Shimadzu, Kyoto, Japan), consisted of an LC-20ADXR pump, an autosampler model Nexera XR Sil-20A, a degasser DGU-20AXR, a column oven CTO-20A and a photodiode array detector model SPD-M20A. Data acquisition was done on a Shimadzu CBM-20A system interfaced with a computer equipped with Shimadzu LC solutions 2.1 software. Separation of α-lapachone, β-lapachone and lapachol was performed on an Eclipse XDB-C18 C18 column (5µm, 150 × 4.6 mm) from Agilent and as mobile phase a mixture of MeOH:$H_2O$:MTBE (60:30:5) at a flow rate of 1mL/min.[31]UV detection was performed at 252nm for α-lapachone (retention time of 2.3 minutes) and at 257nm for β-lapachone (retention time of 2 minutes). The injection volume was 30 µL. Chromatograms obtained at 257 nm are reported in the Supporting Information (Figures S1-S24).

Chromatography analyses: A stock solution of α-lapachone (0.5 mg/mL) was prepared by dissolving 1 mg of α-lapachone in 2 mL of mobile phase. From this stock solution, six calibration solutions were prepared by dilution in mobile phase in the range of 1-20 µg/mL for the construction of an analytical curve used in the quantification of α-lapachone.

A second analytical curve was constructed for the quantification of β-lapachone by the preparation of a stock solution of β-lapachone (0.5 mg/mL) in the mobile phase, and the calibration solutions were in the same range as that used for α-lapachone (1-20 µg/mL).

For the quantification of α-lapachone and β-lapachone under the investigated reaction conditions, the solution was dried under vacuum, and 1 mg of the residual solid was suspended in 1 mL of mobile phase. This solution at 1 mg/mL was diluted to 30 µg/mL in mobile phase and injected into the chromatographic system.

**Determination of the α- and β-lapachone ratio by $^1$H NMR.** $^1$H NMR spectra were recorded on a Varian UNITY plus VXR (500 MHz) spectrophotometer in $CDCl_3$. Integration of the standard $^1$H NMR peaks of the three substances considered in this study (lapachol, α-lapachone and β-lapachone), as shown in Table 3, was used for the quantification of these compounds for each tested experimental condition. The chemical shift values (δ) are given in ppm.

**Table 3.** Chemical shifts used for quantification of the lapachones.

| | δ (Chemical shifts) | |
|---|---|---|
| | $CH_3$ | $CH_2$ |
| α-lapachone | 1.43 | 1.82; 2.62 |
| β-lapachone | 1.47 | 1.85; 2.57 |

*2. Computational methods*

Full geometry optimizations were carried out using the B3LYP functional[32,33] together with the 6-31++G(d,p) basis set.[34,35] Solvation effects were accounted for during the optimization by using water as an implicit solvent in the polarized continuum solvation model (IEFPCM).[36,37] For each optimized stationary point, the second-order Hessian matrix was computed at the same level to confirm the stationary point as a minimum on the potential energy surface, in which all eigenvalues are positive, or a transition structure, with just one negative eigenvalue of the Hessian matrix. For each transition structure, the negative normal mode was animated to confirm that it connects the desired minima. The normal mode calculations were also useful for computing the thermodynamic parameters at 298 K using standard statistical thermodynamic equations for an ideal gas.[38] Empirical scaling of entropies was computed for the multicomponent systems by modifying the standard pressure (P = 1 atm) to a higher pressure, in which the ideal gas would present the same density as liquid water (P = 1354 atm), as proposed by R. L. Martin *et al*. (this procedure only affects the translational part of the entropy by a constant amount so that only free energies of reactions are affected where the particle number changes).[27] The quality of the B3LYP functional for describing the thermodynamic parameters of this class of compounds was tested by comparison of the single point energy calculation with other functionals (N12SX, M06-2X, ωB97X-D, PBE0-D3 and BMK, Figures S40 and S41), and all trends regarding the energy differences on the competitive formation of α- and β-lapachone were compared. For the calculation of the proton affinity and basicity of lapachol, the single-point energies of the optimized structures were calculated at the B3LYP/6-311+G(2df,2p) level including the IEFPCM solvent model. All computations were performed with the G09 software package.[39] Default Gaussian convergence criteria were employed, except for single point calculations, for which a tighter ($10^{-5}$) convergence criterion was used in the SCF.

## Acknowledgements

The authors are grateful to CAPES (*Coordenação de Aperfeiçoamento de Pessoal de Nível Superior*), CNPq (*Conselho Nacional de Desenvolvimento Científico e Tecnológico*), and FAPERJ (*Fundação Carlos Chagas Filho de Amparo à Pesquisa do Estado do Rio de Janeiro*) for funding this research project.

**Keywords:** acidic solution • density functional theory • explicit solvation • lapachol • lapachone

[1] H. Hussain, I. R. Green, *Expert Opin. Ther. Pat.* **2017**, *27*, 1111-1121.
[2] F. C. Silva, V. F. Ferreira, *Curr. Org. Synt.* **2016**, *13*, 334 - 371.
[3] F. Epifano, S. Genovese, S. Fiorito, V. Mathieu, R. Kiss, *Phytochem. Rev.* **2014**, *13*, 37-49.
[4] C. Rios-Luci, E. L. Bonifazi, L. G. Leon, J. C. Montero, G. Burton, A. Pandiella, R. I. Misico, J. M. Padron, *Eur. J. Med. Chem.* **2012**, *53*, 264-274.
[5] E. P. Sacau, A. Estévez-Braun, A. G. Ravelo, E. A. Ferro, H. Tokuda, T. Mukainakac, H. Nishino, *Bioorg. Med. Chem.* **2003**, *11*, 483-488.
[6] Á. G. Ravelo, A. Estévez-Braun, H. Chávez-Orellana, E. Pérez-Sacau, D. Mesa-Siverio, *Curr. Top. Med. Chem.* **2004**, *4*, 241-265.
[7] E. Paternò, *Gazz. Chim. Ital.* **1882**, *12*, 337-392.
[8] S. C. Hooker, *J. Chem. Soc., Trans.* **1892**, *61*, 611-650.
[9] S. C. Hooker, *J. Am. Chem. Soc.* **1936**, *58*, 1190-1197.
[10] M. G. Ettlinger, *J. Am. Chem. Soc.* **1950**, *72*, 3090-3095.
[11] C. Rios-Luci, E. L. Bonifazi, L. G. León, J. C. Montero, G. Burton, A. Pandiella, R. I. Misico, J. M. Padrón, *Eur. J. Med. Chem.* **2012**, *53*, 264-274.
[12] J. Bian, B. Deng, X. Zhang, T. Hu, N. Wang, W. Wang, H. Pei, Y. Xu, H. Chu, X. Li, H. Sun, Q. You, *Tetrahedron Lett.* **2014**, *55*, 1475-1478.
[13] R. Vessecchi, F. S. Emery, N. P. Lopes, S. E. Galembeck, *Rapid. Commun. Mass Spectrom.* **2013**, *27*, 816–824.
[14] J. Tomasi, B. Mennucci, R. Cammi, **2005**, *105*, 2999-3093.
[15] R. E. Skyner, J. L. McDonagh, C. R. Groom, T. van Mourika, J. Mitchell, B. O. *Phys. Chem. Chem. Phys.* **2015**, *17*, 6174-6191.
[16] G.-J. Cheng, X. Zhang, L. W. Chung, L. Xu, Y.-D. Wu, *J. Am. Chem. Soc.* **2015**, *137*, 1706–1725.
[17] R. B. Sunoj, M. Anand, *Phys. Chem. Chem. Phys.* **2012**, *14*, 12715–12736.
[18] Y. Basdogan, J. A. Keith, *Chem. Sci.* **2018**, *9*, 5341-5346.
[19] F. Duarte, J. Åqvist, N. H. Williams, S. C. L. Kamerlin, *J. Am. Chem. Soc.* **2015**, *137*, 1081-1093.
[20] A. V. Marenich, W. Ding, C. J. Cramer, D. G. Truhlar, *J. Phys. Chem. Lett.* **2012**, *3*, 1437-1442.
[21] V. S. Bryantsev, M. S. Diallo, W. A. Goddard III, *J. Phys. Chem. B.* **2008**, *112*, 9709-9719.
[22] C. P. Kelly, C. J. Cramer, D. G. Truhlar, *J. Phys. Chem. A.* **2006**, *110*, 2493-2499.
[23] S. Re, Y. Osamura, K. Morokuma, *J. Phys. Chem. A.* **1999**, *103*, 3535-3547.
[24] C.-G. Ding, K. Laasonen, *Chem. Phys. Lett.* **2004**, *307*, 307-313.
[25] A. D. Hammerich, V. Buch, F. Mohamed, *Chem. Phys. Lett.* **2008**, *460*, 423-431.
[26] A. Gutberlet, G. Schwaab, O. Birer, M. Masia, A. Kaczmarek, H. Forbert, M. Havenith, D. Marx, *Science*. **2009**, *324*, 1545-1548.
[27] Relative Gibbs free energies used for comparison between systems with different number of interacting molecules were corrected for entropy by using standard gas-phase partition functions at 1354 atm, where the ideal gas has the same density as water. See:. R. L. Martin, P. J. Hay, L. R. Pratt, *J. Phys. Chem. A*. **1988**, *102*, 3565-3573.
[28] J. Niskanen, C. J. Sahle, I. Juurinen, J. Koskelo, S. Lehtola, R. Verbeni, H. Müller, M. Hakala, S. Huotari, *J. Phys. Chem. B.* **2015**, *119*, 11732-11739.

[29] C.-G. Dinga, T. Taskilaa, K. Laasonena, A. Laaksonen, *Chem. Phys.* **2003**, *287*, 7-19.
[30] C.-G. Ding, K. Laasonen, A. Laaksonen, *J. Phys. Chem. A.* **2003**, *107*, 8648-8658.
[31] J. Steinert, H. Khalaf, M. Rimpler, *J. Chromatog. A.* **1996**, *723*, 206-209.
[32] A. D. Becke, *J. Chem. Phys.* **1993**, *98*, 5648-5652.
[33] C. Lee, W. Yang, R. G. Parr, *Phys. Rev. B.* **1988**, *37*, 785-789.
[34] J. D. Dill, J. A. Pople, *J. Chem. Phys.* **1975**, *62*, 2921-2923.
[35] M. M. Francl, W. J. Pietro, W. J. Hehre, J. S. Binkley, M. S. Gordon, D. J. DeFrees, J. A. Pople, *J. Chem. Phys.* **1982**, *77*, 3654-3665.
[36] B. Mennucci, E. Cances, J. Tomasi, *J. Phys. Chem. B.* **1997**, *101*, 10506-10517.
[37] J. Tomasi, B. Mennuci, E. Cances, *J. Mol. Struct. (Teochem)*. **1999**, *464*, 211-226.
[38] D. A. McQuarie, J. D. Simon, J. D. in *Physical Chemistry: A Molecular Approach*, University Science Book, California, **1997**.
[39] M. J. Frisch, G. W. Trucks, H. B. Schlegel, G. E. Scuseria, M. A. Robb, J. R. Cheeseman, G. Scalmani, V. Barone, B. Mennucci, G. A. Petersson, H. Nakatsuji, M. Caricato, X. Li, H. P. Hratchian, A. F. Izmaylov, J. Bloino, G. Zheng, J. L. Sonnenberg, M. Hada, M. Ehara, K. Toyota, R. Fukuda, J. Hasegawa, M. Ishida, T. Nakajima, Y. Honda, O. Kitao, H. Nakai, T. Vreven, J. A. Montgomery, Jr., J. E. Peralta, F. Ogliaro, M. Bearpark, J. J. Heyd, E. Brothers, K. N. Kudin, V. N. Staroverov, T. Keith, R. Kobayashi, J. Normand, K. Raghavachari, A. Rendell, J. C. Burant, S. S. Iyengar, J. Tomasi, M. Cossi, N. Rega, J. M. Millam, M. Klene, J. E. Knox, J. B. Cross, V. Bakken, C. Adamo, J. Jaramillo, R. Gomperts, R. E. Stratmann, O. Yazyev, A. J. Austin, R. Cammi, C. Pomelli, J. W. Ochterski, R. L. Martin, K. Morokuma, V. G. Zakrzewski, G. A. Voth, P. Salvador, J. J. Dannenberg, S. Dapprich, A. D. Daniels, O. Farkas, J. B. Foresman, J. V. Ortiz, J. Cioslowski, and D. J. Fox, *Gaussian 09*, revision D.01; Gaussian, Inc.: Wallingford, CT, **2013**.

10.1002/cplu.201800485

WILEY-VCH



# FULL PAPER

Combined experimental and mixed implicit/explicit solvation approaches were employed to obtain insights into the origin of the switchable regioselectivity of acid-catalyzed lapachol cyclization and α-/β-lapachone isomerization. We found that solvating species under distinct experimental conditions stabilized α- and β-lapachone differently, thus altering the identity of the thermodynamic product.

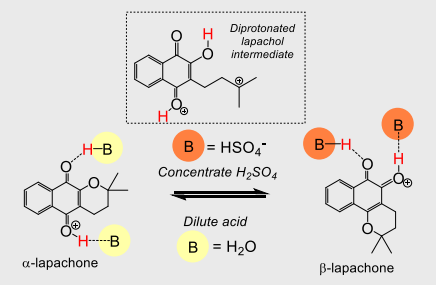


*Maicon Delarmelina, Caroline D. Nicoletti, Marcela C. de Moraes, Debora O. Futuro, Michael Bühl, Fernando de C. da Silva, Vitor F. Ferreira, José W. de M. Carneiro**

***Page No. – Page No.***

**The Conundrum of α- and β-lapachone Isomerization in Acidic Media: Insights from Experimental and Implicit/Explicit Solvation Approaches**